



## Redox hydrogel based immunosensing platform for label-free detection of cancer biomarker

Journal:	<i>Analytical Methods</i>
Manuscript ID:	AY-COM-11-2014-002640.R2
Article Type:	Communication
Date Submitted by the Author:	25-Nov-2014
Complete List of Authors:	Huang, Yaxun; Central South University, surgery, Ding, Yingying; College of Chemistry and Chemical Engineering, Central South University, Li, Ting; Central South University, surgery Yang, Minghui; Central South University, College of Chemistry and Chemical Engineering

1  
2  
3  
4  
5  
6  
7  
8  
9  
10  
11  
12  
13  
14  
15  
16  
17  
18  
19  
20  
21  
22  
23  
24  
25  
26  
27  
28  
29  
30  
31  
32  
33  
34  
35  
36  
37  
38  
39  
40  
41  
42  
43  
44  
45  
46  
47  
48  
49  
50  
51  
52  
53  
54  
55  
56  
57  
58  
59  
60

### Graphical abstract

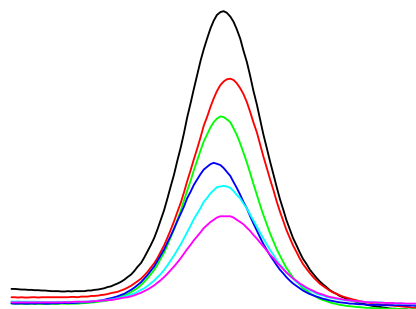


Image of the synthesized hydrogel and square wave voltammetry (SWV) response of the immunosensor to different concentrations of PSA

1  
2  
3  
4 1 Redox hydrogel based immunosensing platform for label-free detection  
5  
6  
7 2 of cancer biomarker  
8  
9  
10 3  
11  
12 4

13  
14 5 Yaxun Huang<sup>a</sup>, Yingying Ding<sup>b</sup>, Ting Li<sup>a\*</sup>, Minghui Yang<sup>b\*</sup>  
15  
16 6

17 7 <sup>a</sup> Department of General Surgery, The Second Xiang-ya Hospital, Central South  
18 8 University, Changsha, 410011 China  
19 9

20 10 <sup>b</sup> College of Chemistry and Chemical Engineering, Central South University,  
21 11 Changsha, China, 410083  
22  
23  
24 12  
25  
26  
27 13  
28  
29  
30 14  
31  
32 15

33  
34 16 Email: [yangminghui@csu.edu.cn](mailto:yangminghui@csu.edu.cn) (M. Yang)  
35 17 Liting850506@163.com (T. Li)  
36 18

37 19 TeL: (+86) 731 88836356  
38 20  
39  
40  
41 21  
42  
43  
44 22  
45  
46  
47 23  
48  
49  
50 24  
51  
52 25  
53  
54  
55 26  
56  
57 27  
58  
59  
60 28

1  
2  
3  
4 29 **Abstract** Redox hydrogel was prepared from ferrocene (Fc) modified amino acid  
5  
6  
7 30 phenylalanine (Phe, F) and utilized to construct an immunosensing platform for the  
8  
9  
10 31 label-free detection of a cancer biomarker prostate specific antigen (PSA). The  
11  
12 32 synthesized hydrogel contains a great number of Fc moieties, which impart the  
13  
14  
15 33 hydrogel with redox properties. The hydrogel modified electrode displays a pair of  
16  
17  
18 34 reversible redox peaks, indicating the facile electron transfer of Fc in the hydrogel at  
19  
20 35 the electrode surface. After the immobilization of the anti-PSA antibody onto the  
21  
22  
23 36 hydrogel modified electrode surface and the capture of PSA molecules, the redox  
24  
25  
26 37 current at the electrode was suppressed significantly due to the blocking of the  
27  
28  
29 38 electron transfer at the electrode surface by the formed immuno-complex. The current  
30  
31 39 change was in proportional to the concentration of PSA detected in the range from 1  
32  
33  
34 40  $\text{pg mL}^{-1}$  to  $10 \text{ ng mL}^{-1}$  with a detection limit of  $0.5 \text{ pg mL}^{-1}$ . The proposed  
35  
36  
37 41 immunosensor is simple with low cost and high sensitivity, which could find wide  
38  
39 42 clinical applications.

40  
41  
42  
43  
44 44 *Keywords:* Ferrocene; Label-free; Phenylalanine; Self-assemble; Redox hydrogel  
45  
46  
47 45  
48  
49  
50 46  
51  
52  
53 47  
54  
55 48  
56  
57  
58 49  
59  
60 50

## 1. Introduction

Immunosensors that are prepared based on the specific binding between antibody and corresponding antigen have found wide applications in clinical diagnosis, food safety testing and environmental monitoring.<sup>1-3</sup> For the successful preparation of immunosensors with good performance, it is crucial to construct the immunosensing platform that could facilitate the immobilization of antibodies and the transduction of immunosensor signals. Different kinds of immunosensing platforms have been reported, such as using nanomaterials (e.g., metal nanoparticles, carbon nanotube, magnetic nanoparticles) to modify the electrode surface.<sup>4-6</sup> These nanomaterials have good biocompatibility and conductivity. While the biocompatibility of these nanomaterials could maintain the activity of the antibodies, the good conductivity of nanomaterials could enhance the electron transfer at the electrode surface. Other methods for the construction of the sensing platform include, but are not limited to, the modification of the electrode with various polymers (e.g., self-assembled monomers and molecularly imprinted polymers) and gels (e.g., silica based sol-gels and hydrogels).<sup>7-10</sup>

By functionalizing gels and hydrogels with different redox moieties, redox hydrogels can be formed.<sup>11, 12</sup> For example, a redox hydrogel is formed by cross-linking poly( N-vinylimidazole) (PVI) complexed to *O*<sub>s</sub>-(4,4'-dimethylbpy)<sub>2</sub>Cl (termed PVI<sub>15</sub>-dmeOs) with poly-(ethylene glycol) diglycidyl ether (PEG).<sup>13</sup> However, the synthesis of such a redox hydrogel is rather complicated and time-consuming. Recently, we discovered stable redox hydrogels could be formed through the

1  
2  
3  
4 73 self-assembly of ferrocene (Fc) modified phenylalanine (Phe, F) monomers (Fc-F) in  
5  
6  
7 74 water.<sup>14, 15</sup> Such prepared hydrogel holds a great number of water molecules, which  
8  
9  
10 75 means the hydrogel has good biocompatibility. The good biocompatibility, plus its  
11  
12 76 facile preparation process and redox functionality enable many applications of the  
13  
14  
15 77 hydrogel in biosensing applications. Biomolecules can either be incorporated into the  
16  
17  
18 78 hydrogel or immobilized on the hydrogel surface.

19  
20 79 In this work, we developed an electrochemical immunosensing platform based on  
21  
22  
23 80 the prepared redox hydrogel for label-free detection of cancer biomarker prostate  
24  
25  
26 81 specific antigen (PSA). PSA has been proved to be the most reliable and specific  
27  
28 82 tumor marker of prostate cancer.<sup>16</sup> Electrochemical methods have the advantage of  
29  
30  
31 83 high sensitivity, low cost and simple instrumentation. The hydrogel modified  
32  
33  
34 84 electrode displays a pair of strong current peaks originated from the Fc moieties in the  
35  
36  
37 85 hydrogel. A chitosan layer was coated onto the hydrogel modified electrode surface to  
38  
39  
40 86 stabilize the hydrogel. Gold nanoparticles (AuNPs) were then adsorbed onto the  
41  
42  
43 87 chitosan layer for the immobilization of anti-PSA antibodies. The specific binding  
44  
45  
46 88 between antibody and PSA resulted in the formation of immuno-complex on the  
47  
48  
49 89 electrode, leading to the decrease of the peak current and quantitative detection of PSA.

## 90 **2. Experimental methods**

### 91 *2.1 Apparatus and reagents*

92 Prostate specific antigen (PSA) and anti-PSA antibody were obtained from  
93  
94  
95  
96  
97  
98  
99  
100 93 Dingguo Biotechnology Co., Ltd. (Beijing, China). Chitosan (MW =140 000-220 000)  
101  
102  
103  
104  
105  
106  
107  
108  
109  
110 94 was purchased from Sigma-Aldrich. Dichloromethane (DCM, ACS grade) used for

1  
2  
3  
4 95 the synthesis was dried and distilled over  $\text{CaH}_2$ , and then stored over molecular sieves.  
5  
6  
7 96 Hydroxybenzotriazole (HOBt), 2-(1H-benzotriazole-1-yl)-1,1,3,3-tetramethyluronium  
8  
9  
10 97 hexafluorophosphate (HBTU), and H-Phe-OMe-HCl were purchased from GL  
11  
12 98 Biochem (Shanghai, China). Ferrocene monocarboxylic acid (Fc-COOH) was  
13  
14  
15 99 obtained from Xiya Reagent (Chengdu, China). For thin layer chromatography, glass  
16  
17  
18 100 plates coated with silica gel (60 GF<sub>254</sub>) were used. For column chromatography, a  
19  
20  
21 101 column with a width of 2.7 cm and a length of 45 cm was packed 18-22 cm high with  
22  
23 102 200-300 mesh silica gel (Silicylcyce, 230-240 mesh). Phosphate buffered saline (PBS,  
24  
25  
26 103 pH 7.4) solution was used as the supporting electrolyte during electrochemical  
27  
28  
29 104 measurements. All other reagents were of analytical grade and deionized water  
30  
31 105 (MillQ, 18.2M $\Omega$ ) was used throughout the study.  
32

33  
34 106 All electrochemical measurements were performed on a CHI 650D electrochemical  
35  
36 107 workstation (Shanghai CH Instruments Co., China). A conventional three-electrode  
37  
38  
39 108 system was used for all electrochemical measurements: a glassy carbon electrode (3  
40  
41  
42 109 mm in diameter) as the working electrode, a saturated calomel electrode as the  
43  
44  
45 110 reference electrode, and a platinum wire electrode as the counter electrode. Scanning  
46  
47  
48 111 electron microscope (SEM) images were obtained from Nova NanoSEM230 (FEI,  
49  
50 112 USA).

### 51 52 113 *2.2 Preparation of the hydrogel*

53  
54  
55 114 The hydrogel was prepared according to our previously reported procedure.<sup>15,</sup>  
56  
57  
58 115 <sup>17</sup>.Fc-COOH (5 mM) and HBTU/HOBt (5.5 mM) were first dissolved in DCM (100  
59  
60 116 mL), and Et<sub>3</sub>N was added dropwise to the solution to activate the carboxyl group.

1  
2  
3  
4 117 After a 1-hour reaction at 0°C, H-Phe-OMe•HCl (5.5 mL) was then added and the  
5  
6  
7 118 reaction mixture was stirred overnight, followed by washing with saturated aqueous  
8  
9  
10 119 solutions of NaHCO<sub>3</sub>, HCl (10%), and water. The resulting solution was then dried  
11  
12 120 over Na<sub>2</sub>SO<sub>4</sub> and evaporated to dryness under reduced pressure. The crude product  
13  
14  
15 121 was purified by flash column chromatography (DCM: EtOAc: PE=3:1:5,v/v/v), and  
16  
17  
18 122 evaporated under reduced pressure in a rotovap to an orange oil. The oil was dissolved  
19  
20 123 in dimethyl sulfoxide (DMSO) and dried in a freeze dryer for overnight, resulting in  
21  
22  
23 124 an orange crystalline solid. The obtained crystalline solid (Fc-Phe-OMe, 3 mM) was  
24  
25  
26 125 dissolved in CH<sub>3</sub>OH (30 mL) and mixed with NaOH (15 mL, 1 M). After being  
27  
28 126 stirred for 2 h, the mixture was neutralized by HCl (10%). After removing the CH<sub>3</sub>OH  
29  
30  
31 127 by evaporation under reduced pressure in a rotovap, an orange suspension was  
32  
33  
34 128 obtained. The suspension was dissolved in DCM followed by washing with HCl (10%)  
35  
36  
37 129 and water, and then dried over Na<sub>2</sub>SO<sub>4</sub>. The crude product was purified by flash  
38  
39 130 column chromatography (DCM: EtOAc: MeOH=9:3:1,v/v/v), then evaporated under  
40  
41  
42 131 reduced pressure in a rotovap to an orange oil. The oil was dissolved in DMSO and  
43  
44  
45 132 dried in a freeze dryer overnight, resulting in an orange needle crystalline solid of  
46  
47 133 Fc-Phe-OH.

48  
49  
50 134 For the preparation of the hydrogel, the lyophilized form of Fc-Phe-OH was  
51  
52 135 dissolved in DMSO at a concentration of 100 mg mL<sup>-1</sup> and used as a stock solution.  
53  
54  
55 136 Then the stock solutions were diluted to a final concentration of 4 mg mL<sup>-1</sup> in PBS  
56  
57  
58 137 (10 mM, pH=7.4) followed by sonication for a few seconds. The suspension turned to  
59  
60 138 clear yellowish hydrogel immediately.

### 139 2.3 Fabrication of the immunosensor

140 To fabricate the immunosensor, 3  $\mu\text{L}$  of hydrogel solution was added onto an  
141 electrode surface. When the electrode was dried, another 3  $\mu\text{L}$  of chitosan solution  
142 (1%, w/w) was applied to the electrode. After the chitosan solution was dried, the  
143 electrode was immersed in an AuNP solution for 1 h to immobilize the AuNPs on the  
144 electrode surface. Then, 3  $\mu\text{L}$  of the antibody ( $10 \mu\text{g mL}^{-1}$ ) solution was added onto  
145 the electrode and incubated for 1 h. After rinsing with PBS solution to remove  
146 non-physically immobilized antibodies, the modified electrode was blocked by  
147 immersing the electrode in 1% BSA solution for 0.5 h. Then, PSA solution of  
148 different concentrations were placed on the electrode surface and incubated for  
149 another 1 h. After rinsing with PBS again, the electrode was ready for measurement.

### 150 3. Results and discussion

151 To prepare the hydrogel, Fc was first coupled onto molecule F (Fc-F). After  
152 dissolving the resulted Fc-F into organic solvent and then the dilution of the stock  
153 solution with phosphate buffer, hydrogel was formed instantly that displays a yellow  
154 color (Figure 1A). The critical gelation concentration (w/w) of Fc-F is about 0.3 ~  
155 0.4 % ( $3 - 4 \text{ mg mL}^{-1}$ ) at room temperature, which means the hydrogel constituted  
156 mainly of water. The synthesized hydrogel was characterized by SEM. As shown in  
157 Figure 1B, the hydrogel was composed of nanofibers. The diameter of the nanofibers  
158 ranged from 50 to 100 nm and the length reached as long as 1 mm. We speculate the  
159 mechanism for the formation of the nanofibers is that Fc-F monomers initially  
160 assembled into dimers, and then the dimers continue to assemble into fibers.<sup>14</sup> The

1  
2  
3  
4 161 inter-fibril interaction contributed to the formation of the hydrogel, and the nanofibers  
5  
6  
7 162 act as an entangled matrix for holding a large amounts of water.<sup>18</sup>  
8

### 163 **Figure 1**

164 The prepared hydrogel was utilized to modify the electrode by directly applying  
165 the hydrogel on an electrode surface. A chitosan layer was then coated on the  
166 electrode to help stabilize the hydrogel. Figure 2A displays 10 successive cyclic  
167 voltammetric scans of the modified electrode in PBS. In these voltammograms, a pair  
168 of well-defined redox peaks at approximately +0.43 and +0.52 V are attributed to the  
169 facile electron transfer of Fc was observed. The strong peak current indicated a  
170 significant number of Fc molecules were incorporated into the hydrogel. In addition,  
171 during the successive scans, no significant current decrease (< 5%) was observed,  
172 indicating good stability of the modified electrode.

173 After demonstrating the strong redox current at the modified electrode, the  
174 electrode was further modified with antibodies for the fabrication of immunosensors  
175 to detect PSA. AuNPs were immobilized on the electrode for the immobilization of  
176 antibodies. Each modification step of the electrode was characterized by cyclic  
177 voltammetry. After the immobilization of antibodies, it can be seen from Figure 2B  
178 (curve a) that the response of the current decreased significantly (55.4% compared to  
179 Figure 2A). When the electrode was further blocked with BSA to minimize non  
180 specific adsorption, the current decreased again (curve b, 73.9% of current decrease  
181 compared to curve a). Finally, when 10 ng mL<sup>-1</sup> of PSA was captured onto the  
182 electrode, there is a continuous decrease of peak current (curve c, 42% of current

1  
2  
3  
4 183 decrease compared to curve b). The electrochemical current was decreased as the  
5  
6  
7 184 formed non-conductive immuo-complex prevented electron transfer at the electrode  
8  
9  
10 185 surface. These data indicated the possibility of the prepared immunosensor for label  
11  
12 186 free detection of PSA.<sup>19, 20</sup>  
13

### 187 **Figure 2**

188 To test the linear range of the immuosensor towards PSA, a series of  
189 immunosensors were prepared for the detection of different concentrations of PSA.  
190 The responses of the immunosensors were measured by square wave voltammetry  
191 (SWV). As expected, the peak current at +0.45 V was decreased as the PSA  
192 concentration increased from 0.001 to 10 ng mL<sup>-1</sup> (Figure 3A). Due to the increase of  
193 PSA concentration, more PSA molecules will be captured onto electrode surface, then  
194 the electrochemical current decreased due to the non-conductive nature of the PSA  
195 molecules. The calibration plot shows good linear relationships between the peak  
196 currents and the logarithm of the PSA concentrations in the range from 1 pg mL<sup>-1</sup> to  
197 10 ng mL<sup>-1</sup> with a correlation coefficient of 0.993 (insert of Figure 3B). The detection  
198 limit, calculated based on S/N = 3, is 0.5 pg mL<sup>-1</sup>. The detection limit is comparable  
199 or lower than literature report, such as the detection of PSA based on nanoporous  
200 silver@carbon dots as labels (0.5 pg mL<sup>-1</sup>)<sup>21</sup>, based on graphene as label ( 1 pg  
201 mL<sup>-1</sup>)<sup>22</sup>, based on ferrocene functionalized iron oxide nanoparticles ( 2 pg mL<sup>-1</sup>)<sup>23</sup>,  
202 and based on quantum dot functionalized graphene sheets as labels (3 pg mL<sup>-1</sup>).<sup>24</sup> In  
203 addition, the developed method is much simpler, which does not require complicated  
204 labeling process.

1  
2  
3  
4 205 The reproducibility of the immunosensor was studied. Five immunosensors were  
5  
6  
7 206 prepared independently for the detection of  $1 \text{ ng mL}^{-1}$  PSA. The relative standard  
8  
9  
10 207 deviation (RSD) of the response currents obtained was within 6%. This shows the  
11  
12 208 reliability of the detection results, indicating the immunosensor can be applied for  
13  
14  
15 209 real-life sample analysis.

16  
17  
18 210 Good selectivity is very important for precise detection of analyte in real-life  
19  
20 211 samples. The selectivity of the proposed immunosensor was investigated. The  
21  
22  
23 212 response of the immunosensor to different other proteins, such as human IgG and  
24  
25  
26 213 human serum albumin (HSA) were tested. As can be seen from Figure 3C, the  
27  
28 214 presence of  $100 \text{ ng mL}^{-1}$  of IgG, HSA and lysozyme do not affect significantly the  
29  
30  
31 215 response of the immunosensor to  $1 \text{ ng mL}^{-1}$  of PSA, indicating good selectivity of the  
32  
33  
34 216 immunosensor.

### 35 36 217 **Figure 3**

37  
38  
39 218 Since the proposed immunosensor displays good selectivity, the immunosensor was  
40  
41  
42 219 then applied for the detection of PSA in serum samples. The diluted human serum  
43  
44  
45 220 samples (1%) were spiked with different concentrations of PSA, and these samples  
46  
47  
48 221 were then tested by the immunosensor. The detected PSA concentration was  
49  
50  
51 222 compared with the concentration of PSA added and the recovery results were obtained.  
52  
53  
54 223 Table 1 shows the recovery results were in the range from 96.9% to 108%, indicating  
55  
56  
57 224 the reliability of the immunosensor results.

## 58 225 **4. Conclusions**

59  
60 226 In this work, we demonstrated an immunosensing platform for label-free detection

1  
2  
3  
4 227 of PSA based on Fc functionalized redox hydrogel. The hydrogel preparation process  
5  
6  
7 228 that based on the self-assemble of Fc-coupled amino acid is simple and efficient. The  
8  
9  
10 229 hydrogel modified electrodes demonstrated strong redox current and good stability.  
11  
12 230 The detection of PSA was achieved through the decrease of the electrode current after  
13  
14  
15 231 the capture of PSA. The resulting immunosensor displays a wide linear range and  
16  
17  
18 232 good selectivity towards PSA detection. The developed immunosensing platform can  
19  
20 233 be easily adapted to develop other immunosensors and find wide clinical applications.  
21  
22

23 234

24  
25 235 **Acknowledgement**  
26

27  
28 236 We are grateful for the support of National Natural Science Foundation of China  
29  
30  
31 237 (21105128, 81200326). The authors thank Dr. Yi Zhang and Mr. Zhifang Sun for help  
32  
33  
34 238 in synthesis of the hydrogel.  
35

36 239

37  
38 240

39  
40  
41 241

42  
43 242

44  
45  
46 243

47  
48  
49 244

50  
51 245

52  
53 246

54  
55  
56 247

57  
58  
59 248  
60

249 **References**

- 1  
2  
3  
4  
5  
6  
7  
8  
9  
10  
11  
12  
13  
14  
15  
16  
17  
18  
19  
20  
21  
22  
23  
24  
25  
26  
27  
28  
29  
30  
31  
32  
33  
34  
35  
36  
37  
38  
39  
40  
41  
42  
43  
44  
45  
46  
47  
48  
49  
50  
51  
52  
53  
54  
55  
56  
57  
58  
59  
60
- 250 1. S. Deng, J. Lei, Y. Huang, Y. Cheng and H. Ju, *Anal. Chem.*, 2013, 85,  
251 5390-5396.
- 252 2. J. F. Rusling, *Anal. Chem.*, 2013, 85, 5304-5310.
- 253 3. M. Yang, S. Sun, Y. Kostov and A. Rasooly, *Sensor. Actuat. B Chem.*, 2011,  
254 153, 176-181.
- 255 4. V. Mani, B.V. Chikkaveeraiah, V. Patel, J. S. Gutkind and J. F. Rusling, *ACS*  
256 *nano*, 2009, 3, 585-594.
- 257 5. M. Yang, H. Li, A. Javadi and S. Gong, *Biomaterials*, 2010, 31, 3281-3286.
- 258 6. H. Li, Q. Wei, G. Wang, M. Yang, F. Qu and Z. Qian, *Biosens. Bioelectron.*,  
259 2011, 26, 3044-3049.
- 260 7. C. Deng, F. Qu, H. Sun and M. Yang, *Sensor. Actuat. B Chem.*, 2011, 160,  
261 471-474.
- 262 8. D. C. Jiang, J. Tang, B. H. Liu, P. Y. Yang and J. L. Kong, *Anal. Chem.*, 2003,  
263 75, 4578-4584.
- 264 9. T. Kitade, K. Kitamura, T. Konishi, S. Takegami, T. Okuno, M. Ishikawa, M.  
265 Wakabayashi, K. Nishikawa and Y. Muramatsu, *Anal. Chem.*, 2004, 76,  
266 6802-6807.
- 267 10. Y. Hou, T. Li, H. Huang, H. Quan, X. Miao and M. Yang, *Sensor. Actuat. B:*  
268 *Chem.*, 2013, 182, 605-609.
- 269 11. B. A. Gregg and A. Heller, *J. Phys. Chem.*, 1991, 95, 5970-5975.
- 270 12. E. J. Calvo and R. Etchenique, *J. phys. Chem. B*, 1999, 103, 8944-8950.

- 1  
2  
3  
4 271 13. T. J. Ohara, R. RaJagopala and A. Heller, *Anal. Chem.*, 1994, 2451-2457.  
5  
6  
7 272 14. Z. F. Sun, Z. Y. Li, Y. H. He, R. J. Shen, L. Deng, Y. Z. Liang and Y. Zhang, *J.*  
8  
9 273 *Am. Chem. Soc.*, 2013, 135, 13379-13386.  
10  
11  
12 274 15. F. L. Qu, Y. Zhang, A. Rasooly and M. H. Yang, *Anal. Chem.*, 2014, 86,  
13  
14 275 973-976.  
15  
16  
17 276 16. H. Lilja, A. Chrstensson, U. Dahlén, M. T. Matlkainen, O. Nilsson, K.  
18  
19 277 Pettersson and T. Lovgren, *Clin. Chem.*, 1991, 37, 1618-1625.  
20  
21  
22 278 17. M. Zhou, Z. Sun, C. Shen, Z. Li, Y. Zhang and M. Yang, *Biosens. Bioelectron.*,  
23  
24 279 2013, 49, 243-248.  
25  
26  
27 280 18. A.M. Smith, R.J. Williams, C. Tang, P. Coppo, R.F. Collins, M.L. Turner, A.  
28  
29 281 Saiani and R. V. Ulijn, *Adv. Mater.*, 2008, 20, 37-41.  
30  
31  
32 282 19. Q. Wei, K. Mao, D. Wu, Y. Dai, J. Yang, B. Du, M. Yang and H. Li, *Sensor.*  
33  
34 283 *Actuat. B Chem.*, 2010, 149, 314-318.  
35  
36  
37 284 20. Q. Wei, Y. Zhao, C. Xu, D. Wu, Y. Cai, J. He, H. Li, B. Du and M. Yang,  
38  
39 285 *Biosens. Bioelectron.*, 2011, 26, 3714-3718.  
40  
41  
42 286 21. L. D. Wu, M. Li, M. ZHANG, M. Yan, S. H. Ge and J. H. Yu, *Sensor. Actuat. B*  
43  
44 287 *Chem.*, 2013, 186, 761-767.  
45  
46  
47 288 22. M. H. Yang, A. Javadi, H. Li and S. Q. Gong, *Biosensor.Bioelectron.*, 2010, 26,  
48  
49 289 560-565.  
50  
51  
52 290 23. H. Li, Q. Wei, J. He, T. Li, Y. F. Zhao, Y. Y. Cai, B. Du, Z. Y. Qian and M. H.  
53  
54 291 Yang, *Biosensor.Bioelectron.*, 2011, 26, 3590-3595.  
55  
56  
57 292 24. M. H. yang, A. Javadi and S. Q. Gong, *Sensor. Actuat. B Chem.*, 2011, 155,  
58  
59  
60

1		
2		
3		
4	293	357-360.
5		
6		
7	294	
8		
9		
10	295	
11		
12	296	
13		
14		
15	297	
16		
17		
18	298	
19		
20	299	
21		
22		
23	300	
24		
25		
26	301	
27		
28	302	
29		
30		
31	303	
32		
33		
34	304	
35		
36	305	
37		
38		
39	306	
40		
41		
42	307	
43		
44		
45	308	
46		
47	309	
48		
49		
50	310	
51		
52	311	
53		
54		
55	312	
56		
57		
58	313	
59		
60	314	

1  
2  
3  
4 315 **Figure captions:**  
5

6  
7 316 Figure 1. (A) Image of the synthesized hydrogel, (B) SEM characterization of the  
8  
9 317 hydrogel.

10  
11 318 Figure 2. (A) Ten successive cyclic voltammetry curve of the hydrogel modified  
12  
13 319 electrode in buffer. (B) Cyclic voltammetry response of the immunosensor after  
14  
15 320 different modification steps, (a) after antibody ( $10 \mu\text{g mL}^{-1}$ ) immobilization, (b)  
16  
17 321 after BSA (1%, w/w) blocking, (c) after the capture of PSA ( $10 \text{ ng mL}^{-1}$ ). Scan  
18  
19 322 rate, 0.1 V/s.

20  
21 323 Figure 3. (A) Square wave voltammetry (SWV) response of the immunosensor to  
22  
23 324 different concentrations of PSA, from a to f, 0, 0.001, 0.01, 0.1, 1, 10  $\text{ng mL}^{-1}$ .  
24  
25 325 The parameters for SWV were as follows: potential increment of 4 mV, pulse  
26  
27 326 amplitude of 25 mV and frequency of 15 Hz. (B) Calibration curve of the  
28  
29 327 immunosensor to different concentrations of PSA. (C) Response of the  
30  
31 328 immunosensor to different samples. The concentration of PSA is  $1 \text{ ng mL}^{-1}$  and  
32  
33 329 the concentration of interfering proteins is  $100 \text{ ng mL}^{-1}$ . Error bar = SD, n=3.  
34  
35

36  
37 330  
38

39  
40 331  
41

42  
43 332  
44

45  
46 333  
47

48  
49 334  
50

51  
52 335  
53

54  
55 336  
56  
57  
58  
59  
60

1  
2  
3  
4  
5  
6  
7  
8  
9  
10  
11  
12  
13  
14  
15  
16  
17  
18  
19  
20  
21  
22  
23  
24  
25  
26  
27  
28  
29  
30  
31  
32  
33  
34  
35  
36  
37  
38  
39  
40  
41  
42  
43  
44  
45  
46  
47  
48  
49  
50  
51  
52  
53  
54  
55  
56  
57  
58  
59  
60

337

338

339

340

341

342 Table 1 Recovery of the PSA concentration in human serum samples (n= 3)

Sample No.	1	2	3	4
Amount of PSA added( $\text{pg mL}^{-1}$ )	10	100	1000	10000
Amount of PSA detected( $\text{pg mL}^{-1}$ )	9.69 $\pm$ 0.540	108 $\pm$ 5.17	1026 $\pm$ 43.2	10020 $\pm$ 472
Recovery (%)	96.9 $\pm$ 0.540	108 $\pm$ 0.517	102 $\pm$ 0.432	100 $\pm$ 0.472

343

344

345

346

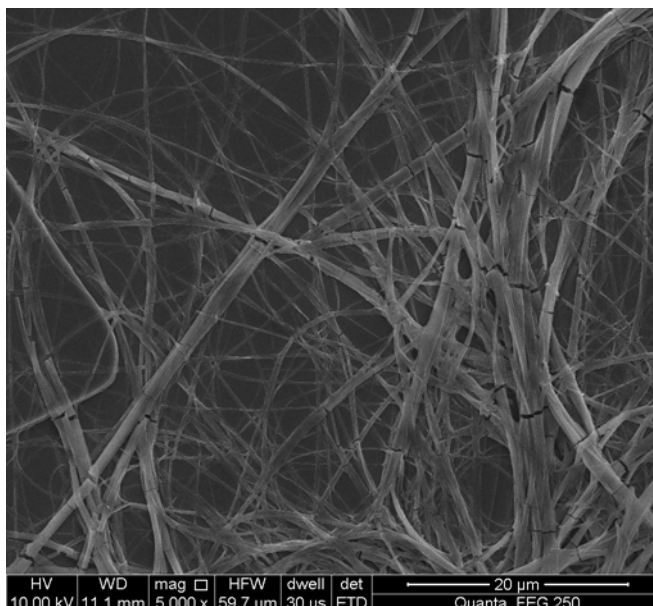
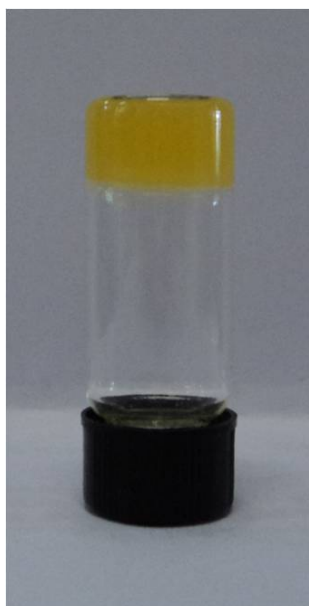
347

348

349

350

351

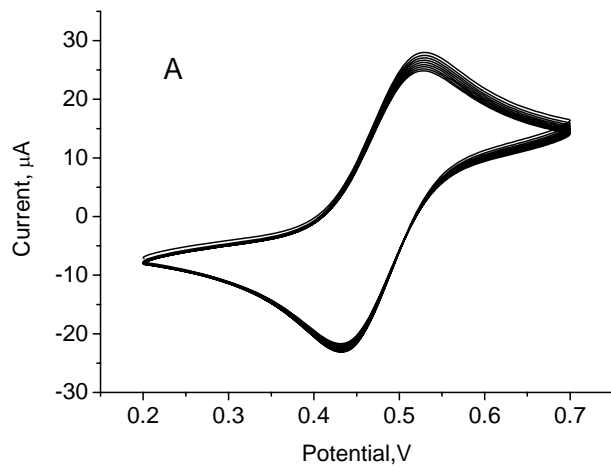


(A)

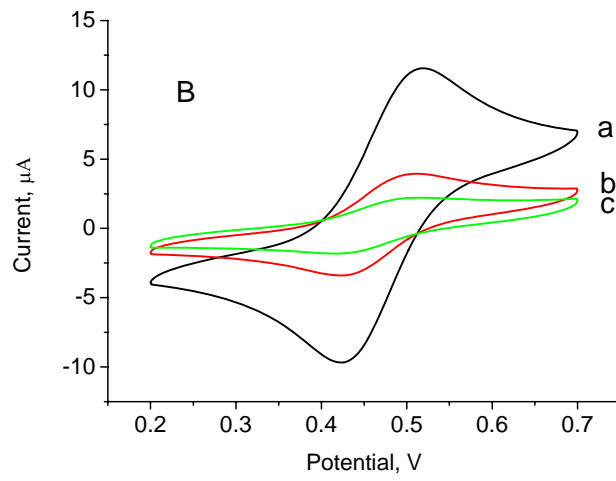
(B)

Figure 1

352  
353  
354  
355  
356  
357  
358  
359  
360  
361



362



363

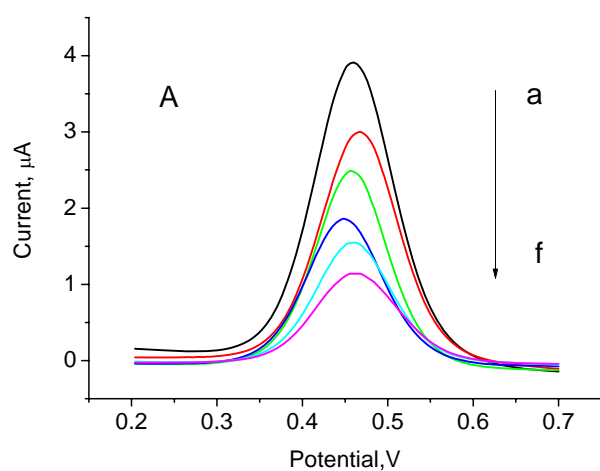
364

**Figure 2**

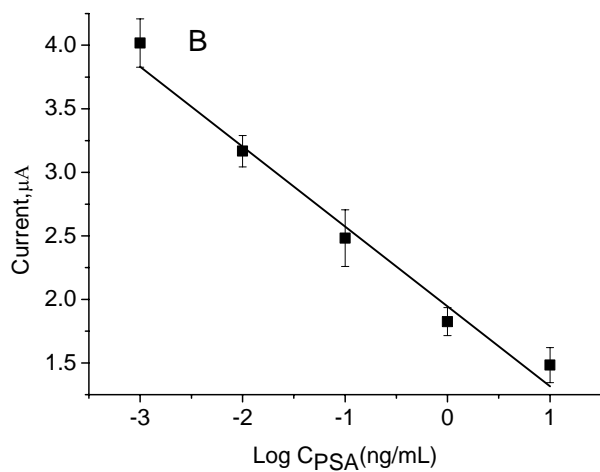
365

366

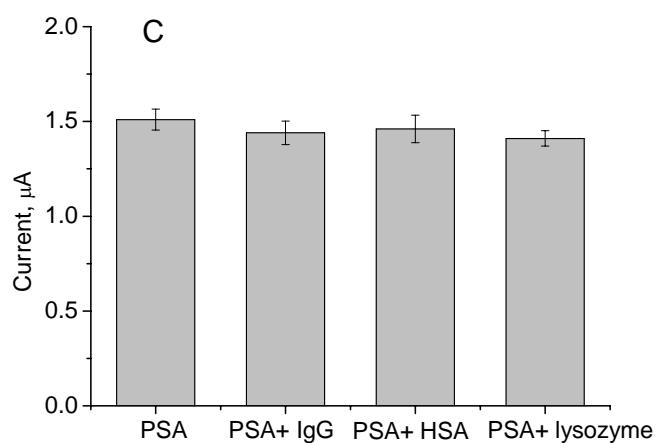
367



368



369



370

371

**Figure 3**

372

373